Carbohydrate Polymers 93 (2013) 484–491

Contents lists available at SciVerse ScienceDirect

Carbohydrate Polymers

journal homepage: www.elsevier.com/locate/carbpol

Electrospinning of commercial guar-gum: Effects of purification and filtration

Adriana F. Lubambo[a,b,*], Rilton A. de Freitas[b], Maria-R. Sierakowski[b], Neoli Lucyszyn[b,d], Guilherme L. Sassaki[c], Bruno M. Serafim[a], Cyro Ketzer Saul[a]

[a] LITS, Physics Department, Universidade Federal do Paraná, P.O. Box 19044, Centro Politecnico, Curitiba, Brazil
[b] BioPol, Chemistry Department, Universidade Federal do Paraná, P.O. Box 19081, Centro Politécnico, Curitiba, Brazil
[c] Biochemisty Department, Universidade Federal do Paraná, P.O. Box 19046, Centro Politécnico, Curitiba, Brazil
[d] Chemistry Department, School of Educational Humanities, Pontifícia Universidade Católica do Paraná, PUCPR, Campus Curitiba, Brazil

ARTICLE INFO

Article history:
Received 22 October 2012
Received in revised form
11 December 2012
Accepted 13 January 2013
Available online 23 January 2013

Keywords:
Electrospinning
Galactomannans
Aggregation
Purification
Membrane filtration

ABSTRACT

Guar gums of two different commercial sources were successfully electrospun on both mica and copper tape at several concentrations starting from 1% (w/w). The electrospun fibers formed with the raw materials were not uniform and presented aggregates and beads within the fibers. Two different purification procedures and a filtration sequence with different pore size membranes were applied to enhance galactomannan solution homogeneity and solubility. The consequence was improved fiber morphology. We observed that the precipitation step, within the purification procedure, produced changes in the molar mass distribution and yielded different fiber diameter. Furthermore, spherical aggregates between fibers and within them disappeared after the sequential filtration. The resulting electrospun fiber diameter decreased with membrane pore diameter reduction. We conclude that the filtration process is responsible for molecular disentanglement, as well as disaggregation, which leads to improved electrospun galactomannan fiber morphology.

1. Introduction

The use of polysaccharides from plants and seeds in innovative biopolymer technologies is of key importance. The reason relies on their intrinsic properties, abundant natural origin and renewability (Schiffman & Schauer, 2008). The fact that they can be degraded by microorganisms turns them into environmental friendly materials replacing with advantages their fuel consuming synthetic counterparts (Simkovic, 2008). Intrinsic properties, like biocompatibility, high porosity, and controllable mechanical properties enable them to mimic the extracellular matrix with high efficiency (Agarwal, Wendorff, & Greiner, 2008; Lee, Jeong, Kang, Lee, & Park, 2009). Therefore, they are very suitable for applications in regenerative medicine, tissue engineering, wound dressing and as immobilization matrix for signaling and bio-catalysis (Agarwal et al., 2008). They can also provide scaffold for cell regeneration, without stimulating immune responses, and in some cases to have anti-bacterial properties, which help wound healing (Agarwal et al., 2008; Lee et al., 2009).

One important requirement of biocompatibility and biodegradability for devices which mimic extra cellular matrix and allow cell proliferation is their degradation time. After degradation they open space for new cells or tissues. Those devices must also be formed by highly porous 3D loose mats with high surface area to allow cell binding and spread. If their structure present features at the nanoscale, it implies in higher surface area and therefore more binding sites for cell membrane receptors (Agarwal et al., 2008).

Among the classical methods to produce nanofibers like phase separation (Ma & Zhang, 1999) are island in the sea (Nakata et al., 2007); drawing (Ondarçuhu & Joachim, 1998); template synthesis (Duvail et al., 2002); self–assembly (Liu et al., 2002) and electrospinning (Greiner & Wendorff, 2007). Electrospinning is a suitable candidate for producing mats for tissue regeneration because of its ability to produce fibers at nanoscale at low cost and with a large variety of materials. However, few polysaccharides have been electrospinned to date (Lee et al., 2009), among then we find the following most common electrospun polysaccharides: cellulose, cellulose acetate, cellulose composites, chitosan and alginate. One reason for such a few successfully electrospun polysaccharides has its origin in the challenge of tuning their electrospinning parameters, which are unique for each polymer (Schiffman & Schauer, 2008). Differences arise from their physicochemical properties, like molecular weight; degree of de-acetylation; purity; charged groups distribution; gelling behavior and surface tension, which depend on the polysaccharide source (Schiffman & Schauer, 2008). This

* Corresponding author at: UFPR, Av. Cel. Francisco H. dos Santos, Centro Politécnico, Jardim das Américas, 81531-990 Curitiba-PR, Brazil. Tel.: +55 41 33613092; fax: +55 41 33613418.
E-mail addresses: af.lubambo@uol.com.br, af.lubambo@gmail.com (A.F. Lubambo).

0144-8617/$ – see front matter © 2013 Published by Elsevier Ltd.
http://dx.doi.org/10.1016/j.carbpol.2013.01.031

can be an obstacle for producing controllable and homogeneous fiber networks, requiring unique conditions for each production batch. Nonetheless, the final benefit from their unique properties can largely exceed these restrictions.

In this work we address the issue of producing nanofibers networks as well as the enhancement of fiber homogeneity using commercial guar gums, from two different sources. It is believed in the literature that this polysaccharide alone does not form fibers, only droplets (Stijnman, Bodnar, & Tromp, 2011). In fact, to the best of our knowledge, guar gum is related to fiber formation only in association with synthetic polymers which improve dilute solution electrospinnability by modulating rheological properties (Talwar, Hinestroza, Pourdeyhimi, & Khan, 2008).

Guar gums, also known as galactomannans, are neutral polysaccharides extracted of the seed endosperm of leguminosaes whose structure is formed by a linear (1–4)-β-linked backbone of mannose units, with side chains of single galactose (Pollard et al., 2008). The ratio (Mannose:Galactose) in this polysaccharide defines the degree of galactose substitution which is responsible for synergetic interactions and solubility. A high degree of substitution is linked to higher solubility due to better hydration near the galactose regions (Bourbon et al., 2010; Mccleary, Amado, Warbel, & Neukom, 1981). Guar gum has a high degree of substitution as for example, ~1.6–1.8:1 (Cheng, Prud'homme, Chik, & Rau, 2002). Also, it is possible to find guar gums with degrees of 1.2 (Ganter, Milas, Corrêa, Reicher, & Rinaudo, 1992) which are very soluble.

During electrospinning, the uniformity of the fibers depends on many parameters. Among solution parameters are viscosity; polymer concentration; polymer molar mass; electrical conductivity; elasticity and surface tension (Greiner & Wendorff, 2007). However, as pointed out by (Shenoy, Bates, Frisch, & Wnek, 2005), not all parameters are fundamental or independent. In some instances, the uniformity is the consequence of the improvement of more than one parameter. Nonetheless, it is also possible that among all parameters, a few may dominate and have a first order influence in the uniformity of fibers.

The ability to form uniform fibers, instead of beads, can be largely dependent of chain entanglements during electrospinning as seen in Gupta and Wilkes (2003); Kenawy et al. (2003); and Shenoy et al. (2005). Furthermore, recently, increasing chain entanglement was pointed out as responsible for successful electrospinning of alginate, a linear polysaccharide which does not form nanofibers in water solution (Nie et al., 2008). Improvement in chain entanglement and conformation, both dominant parameters associated with increasing conductivity and viscosity were responsible for uniform fiber formation. On the other hand, entanglement and aggregation, in some cases, can cause the opposite effect. It can lead to polysaccharide chain stiffening and solubility reduction (Lang & Kajiwara, 1993; Li, Wan, Cui, Huang, & Kakuda, 2006; Picout, Ross-Murphy, Errington, & Harding, 2003; Vårum, Smidsrød & Brant, 1992), which are undesirable effects for electrospinning.

In this work we were able to enhance fiber homogeneity of electrospun guar gums, by improving solution parameters like solubility and aggregation reduction. In fact, it is known that insoluble residues are present in commercial guar gums favoring aggregation. Insoluble residues have its origin on the final milled endosperm which contains around 2.5% of crude fiber, 10–15% of moisture, 5–6% of protein and 0.5–0.8% of ash (Mark et al., 2007). Even after purification, aggregation can still occur for two reasons: the remaining presence of extraction residues, which depends on the purification method (Cunha, de Paula, & Feitosa, 2007); and a remaining degree of entanglement that always occurs because galactomannan molecules interact with each other through hydroxyl groups. Galactomannans are also known to present "hyperentanglements" (Newlin, Lovell, Saunders, & Ferry, 1962; Robinson, Ross-Murphy, & Morris, 1982; Wientjes, Duits, Jongschaap, & Mellema, 2000). Such features are described by Gittings et al. (2000) not as entangled chains, but as supramolecular aggregate structures with more than one chain, whose size increases with the concentration. The quantity of aggregates and its size will depend mainly on the drying process (Pollard et al., 2008; Wang, Huang, Nakamura, Burchard, & Hallet, 2005). There are several physical methods for disentanglement or disaggregation of chains like warming, centrifugation and filtration (Gomez, Navarro, Manzanares, Horta, & Carbonell, 1997). In this work, we used a sequence of membrane filtration with decreasing pore size to enhance fiber homogeneity.

2. Materials and methods

2.1. Polysaccharide

Commercial guar gum was supplied by Biotec (batch no. 21038, Brazil) with molar weight (M_w: 0.519×10^6 g/mol) and by Sigma–Aldrich (batch no. 100M0221V, India) with molar weight (M_w: 3.896×10^6 g/mol).

2.2. Purification procedure

Guar gum was purified as following: the commercial powder was solubilized in purified water (Milli-Q System-Millipore) at 25 °C and stirred overnight. Then, it was centrifuged at 10,375*g* at the temperature of 40 °C for 1 h. The supernatant was precipitated by two different procedures using two volumes of ethanol (95%, v/v).

Procedure 1. Supernatant was poured into ethanol which leaded to Sigma A (GGS-AP) and Biotec A (GGB-AP).
Procedure 2. Ethanol was poured into the supernatant which leaded to Sigma B (GGS-BP) and Biotec B (GGB-BP).

Then each one was filtered through cloth and washed with ethanol three times. The obtained product was collected and slightly milled before drying at 40 °C for 2 days. After drying, each product was milled again to produce a fine powder ready to use.

2.3. Filtration

The polysaccharide solutions (1 mg/ml) were filtered sequentially through a series of Millipore® cellulose ester membranes with 3.0, 0.8, 0.45, 0.22 μm decreasing pore diameters. After each membrane filtration, aliquots were immediately taken for analysis by time dependent static light scattering (TDSLS). Measurements were performed in recirculation mode, at 0.5 ml/min, using a Shimadzu pump 20A coupled to 90° static light scattering (LS), viscometer (VIS) and refraction index measurement (RI), all from Viscotek. The effect of filtration pore size on aggregation, relative viscosity and recovery concentration were determined by averaging 5000 points. After the last membrane filtration (0.22 μm) the aggregate average diameter was monitored during 1 h without detectable change. Electrospinning experiments were performed with these samples within 1 h to assure stability.

2.4. Protein content determination

Protein content was determined accordingly to (Hartree, 1972), using the Folin-Ciocalteau reagent (Merck®) and, a standard reference curve with Sigma Albumin, (batch no. 017KO722). The analysis was performed in a Biospectro spectrophotometer, model SSP-200 in a 1 cm long quartz cuvette.

2.5. Electrospinning

The positive terminal of a high voltage power supply (0–40 kV) was attached to a 0.7 mm blunt chirurgical needle which worked as the metallic capillary. The polysaccharide solution was loaded into a 2.5 ml Hamilton syringe and pumped with a syringe pump at 6.7–15.8 μl/min flow rates. The tip to collector distance varied within 2.5–20 cm. The parameters (voltage, flow rate and tip-collector distance) were adjusted to obtain a stable Taylor cone during the electrospinning process. We used both mica and copper double side tape as substrates which were attached on top of a grounded aluminum collector plate.

2.6. Gel permeation chromatography

The GPC experiments were performed with a Viscotek-GPC multi-detector-system equipped with an OH-Pack Shodex SB-806 M HQ with size exclusion limits of 2×10^7 g/mol and coupled to a RI Viscotec model (VE3580), using sodium nitrate 0.1 mol/l containing 200 ppm of azide as eluent.

The polysaccharide solution with 1 mg/ml concentration was solubilized with purified water (Milli-Q System-Millipore) overnight and filtered through a 0.22 μm cellulose membrane prior to injection. The 100 μl solution samples were injected into the GPC system to determine the average molar mass (M_w), intrinsic viscosity $[\eta]_w$, polydispersity index (M_w/M_n), column recovery, and Mark-Houwink constant (α). Results were analyzed with OmniSEC software (Malvern. Co., USA). The measured refractive index increment value (dn/dc) was 0.132 for Sigma and 0.124 for Biotec.

2.7. Atomic force microscopy (AFM)

AFM imaging was performed using a commercial Shimadzu SPM-9500J3 microscope at room temperature (~24 °C). Images were taken in dynamic tapping mode (TM-AFM) with an oxide-sharpened micro-fabricated silicon cantilever (μ-Masch) with a nominal spring constant of 4.7 N/m. Some samples were scanned with a 40 N/m cantilever with a less than 10 nm tip radius of curvature. The scanning rate was 1 Hz and the image resolution was 256 × 256 pixels. The operating point was adjusted to minimize the interaction between the tip and sample to avoid layer deformation. After acquisition, image treatment was performed using Shimadzu software for flattening.

2.8. NMR spectroscopy

The samples (20 mg/ml) were deuterium exchanged by repeated dissolution in D_2O followed by freeze-drying (3 times). Spectra were obtained at 70 °C, using TMSP-d4 (2,2,3,3-tetradeuterium-3-trimethylilsilylpropionate) as standard ($\delta = 0$). All spectra were obtained with a Bruker 400 MHz AVANCE III NMR spectrometer with a 5 mm inverse gradient probe. 1D 1H-NMR were performed after 90° (p1) pulse calibration by evolution until 360° using a start p1 of 4 μs plus increment of 2 μs (p1 7.0–9.1 μs), calculation of offset (1885.0–1885.6 Hz) to obtain a spectrum width of 8012.8 Hz. It corresponds to an oversampling of 8× fold to the carbohydrate region, using 128 scans to give a signal/noise (S/N) ratio of at least 1400/1 for the anomeric region (90° pulse, relaxation delay = 10.0 s, number of time domain points = 32,768 and acquisition time = 2.0447 s). Integration of H-1 areas belonging to mannose and galactose units was performed without tube rotation and respecting a HDO signal with a medium half line width varying from 1.7 to 2.5 Hz after Lorentzian deconvolution and post Fourier transformation (Sassaki et al., 2011).

3. Results and discussions

3.1. Biotec guar gum (GGB)

GPC results, on Table 1, show that the purification procedure applied on commercial samples changed very slightly the average molar mass as well as intrinsic viscosity. Polydispersity index did not change for purified samples. This polysaccharide has a flexible chain conformation, with Mark-Houwink α exponent lying in the 0.5–0.8 interval, which is characteristic of random flexible coil, and comparable to earlier works (Robinson et al., 1982).

3.1.1. Non-purified Biotec guar gum (GGB-NP)

Non purified Biotec guar gum (GGB-NP) was electrospun using different solution concentrations on mica as seen in Fig. 1A–C. It is possible to see that fibers were produced together with spherical aggregates. The presence of aggregates can be due to insoluble aggregates in suspension, originated from residues coming from the milled endosperm. After purification the dried content of residue, and purified guar were weighted. Approximately 8.9% (w/w) consisted of insoluble residues.

3.1.2. Purified Biotec guar gum (GGB-P)

Figs. 1D–F and 2C show GGB-AP networks of fibers using purification procedure 1 for two different solution concentrations, 3% and 1% (w/w). Even after purification a very few spherical aggregates can still be observed. Also, it was possible to notice that the electric field needed to obtain the electrospun fibers after purification decreased approximately 3 times.

3.1.2.1. Purified GGB-AP filtered successively through decreasing pore size. GGB-NP was purified and filtered by a series of cellulose membranes with decreasing pore sizes. We noticed a solution conductivity drop, as well as a protein content reduction after solution purification. The results in Fig. 2 show that the fiber homogeneity was enhanced with filtration. On the GGB-AP sample only a few aggregates, smaller than the ones seen in Fig. 2C, were still present, as in Fig. 2I. It was also observed that smaller membrane pores leaded to smaller fiber diameters, as seen in Table 2. The measured fiber diameter in Table 2 is overestimated due to the tip convolution effect. The deconvoluted fiber diameter was calculated accordingly to Engel, Schoenenberger, and Müller (1997) with the assumption that the AFM tip radius of curvature $r = 10$ nm. Conductivity remained slightly the same during the filtering process which suggests no further protein removal.

Using TDSLS-RI-VIS, the RI signals allowed concentration evaluation and thus the filtration material loss using 3.0, 0.8, 0.45 and 0.22 μm Millipore filters. The graphs of Fig. 3A and B show that there is a negligible change in RI signal and less than 8% material loss after 0.22 μm filtration for Sigma B. By contrast, filtration has a significant effect on LS signal. LS intensity, seen in Fig. 3A for Biotec A samples, is due to both isolated macromolecules and aggregates. After filtering through 3.0, 0.8, 0.45 and 0.22 μm, there is an apparent linear drop in LS signal, meaning a reduction of aggregate average diameter. However it was not observed similar drop in protein content neither in conductivity. Therefore we assume that the drop of LS signal is due to disaggregation. Furthermore, the relative viscosity showed to be independent of filtration, as seen in Fig. 3A and B, which is in agreement with Freitas, Drenski, Alb, and Reed (2010). Sigma B samples presented the same behavior after filtration. Consequently, we can associate disaggregation to both fiber diameter reduction and elimination of aggregates.

3.1.2.2. NMR results. NMR results indicate that purification and filtration did not influence the Man:Gal (Mannose:Galactose) ratio peaks located at δ 5.2 ppm and δ 5.5 ppm respectively. In fact, the

Table 1
Physico-chemical properties evaluated by GPC for purified, non-purified Biotec and purified, non-purified Sigma guar gum.

Sample	M_w (g/mol)	M_w/M_n	R_h (nm)	R_g (nm)	[η] (dl/g)	c^* (g/ml)	α	Column recovery (%)
Biotec								
GGB-NP	519,475	1.6	31.8	55.0	4.33	1.23×10^{-3}	0.6	89
GGB-AP	430,244	1.6	29.3	51.6	4.13	1.24×10^{-3}	0.6	100
GGB-BP	442,562	1.6	29.8	51.0	4.20	1.32×10^{-3}	0.6	91
Sigma								
GGS-NP	3.896×10^6	15.6	–	–	–	–	–	46
GGS-AP	1.009×10^6	2.7	42.8	67.6	5.85	1.29×10^{-3}	0.5	100
GGS-BP	1.036×10^6	2.5	44.0	70.3	6.20	1.18×10^{-3}	0.5	95

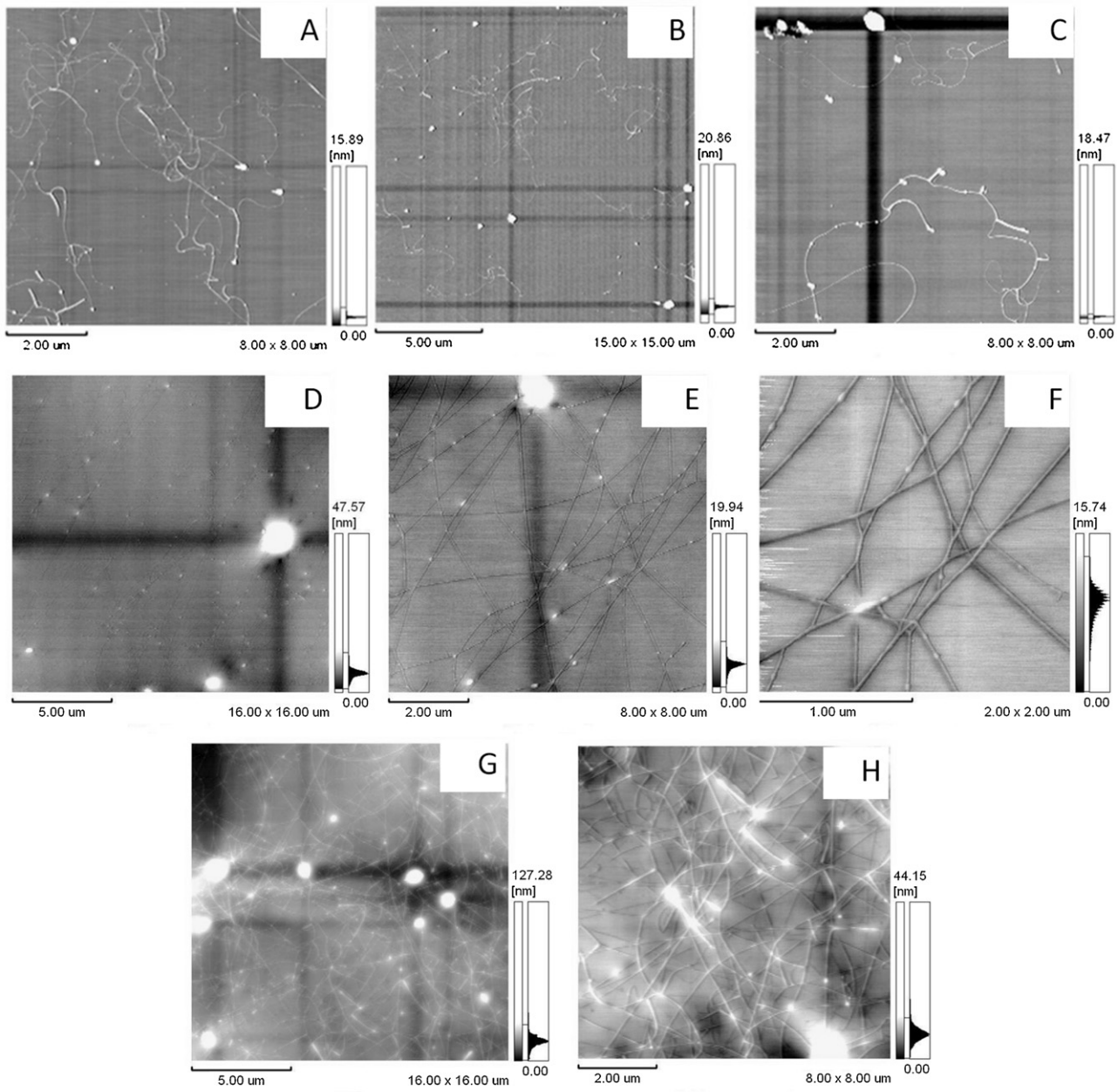

Fig. 1. AFM images in dynamic mode of nano-fiber network of non-purified Biotec guar gum obtained on mica at different concentrations of guar: (A) GGB-NP (8.00 × 8.00) μm, 1.6% (w/w), 4 kV/cm, 15.6 μl/min; (B) GGB-NP (15.00 × 15.00) μm, 1.8% (w/w), 4.68 kV/cm, 13.9 μl/min; (C) GGB-NP (8.00 × 8.00) μm, 2.0% (w/w), 4.68 kV/cm, 15.8 μl/min. AFM images in dynamic mode of nano-fiber network of purified Biotec guar gum on copper double-tape: (D) GGB-AP (16.00 × 16.00) μm, 3% (w/w), 1.6 kV/cm, 6.7 μl/min feed rate; (E) GGB-AP, zoom of image (D) (8.00 × 8.00) μm; (F) GGB-AP, zoom of image (E), (2.00 × 2.00) μm. AFM images in dynamic mode of nano-fiber network of non-purified Sigma guar gum on copper double-tape: (G) GGS-NP (16.00 × 16.00) μm, 1% (w/w) deposited by electrospinning; (H) zoom of image (G). Experimental conditions: (G) 0.56 kV/cm, feed rate 10.2 μl/min.

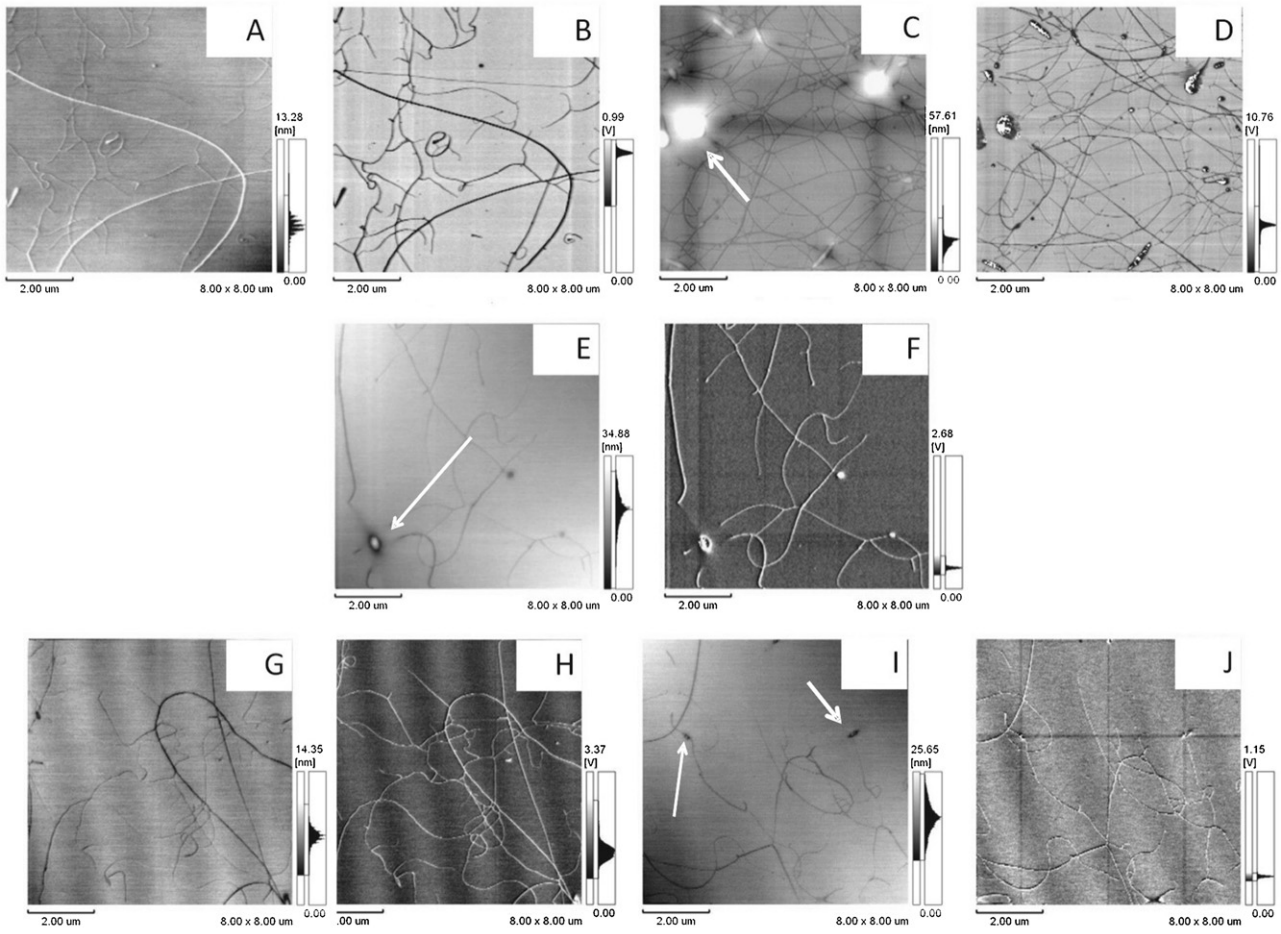

Fig. 2. AFM images of GGB 1% (w/w) electrospun fibers on copper double-tape. (A) GGB-NP, 1% (w/w), (8.00 × 8.00) μm. (B) GGB-NP, phase image of A, (8.00 × 8.00) μm. (C) GGB-AP purified, 1% (w/w), (8.00 × 8.00) μm. (D) GGB-AP, phase image of C, (8.00 × 8.00) μm. (E) GGB-AP filtered with 0.8 μm pore cellulose membrane (8.00 × 8.00) μm. (F) GGB-AP (8.00 × 8.00) μm, phase image of (E). (G) GGB-AP filtered with 0.45 μm pore cellulose membrane (8.00 × 8.00) μm. (H) GGB-AP, phase image of (G) (8.00 × 8.00) μm. (I) GGB-AP filtered with 0.22 μm pore cellulose membrane (8.00 × 8.00) μm. (J) GGB-AP, phase image of (I) (8.00 × 8.00) μm. Experimental conditions for (A), (C) 0.52 kV/cm, feed rate 9.3 μl/min. (E), (G), (I) 0.42 kV/cm, feed rate 9.3 μl/min.

Table 2
Average diameter D (nm), deconvoluted diameter D^* (nm), conductivity C (μS/cm) and protein content P % (w/w) for non-purified, purified, purified and filtered GGB and GGS guar gum.

Sample Biotec	D (nm)	δD (nm)	D^* (nm)	Conductivity ($C \pm 1.1$) (μS/cm)	Protein content ($P \pm 0.1$)% (w/w)
	1% (w/w)			0.1% (w/w)	
GGB-NP	78.2	16.7	60.7	19.7	4.0
GGB-AP	63.8	18.5	47.0	6.6	1.6
GGB-3.0AP	–	–	–	6.6	1.0
GGB-0.8AP	63.0	17.3	46.0	6.6	0.8
GGB-0.45AP	51.4	12.8	35.1	6.6	0.7
GGB-0.22AP	40.0	17.2	24.6	6.6	0.7
Sample Sigma	D (nm)	δD (nm)	D^* (nm)	Conductivity ($C \pm 1.9$) (μS/cm)	Protein content ($P \pm 0.1$) % (w/w)
	1%(w/w)			0.1% (w/w)	
GGS-NP	–	–	–	18.1	4.1
GGS-AP	54.7	12.2	38.2	6.9	2.7
GGS-BP	91.1	23.2	73.3	8.1	2.2
GGS-3.0BP	–	–	–	8.1	1.2
GGS-0.8BP	86.5	33.0	68.7	8.1	0.9
GGS-0.45BP	73.6	22.5	56.2	8.1	0.9
GGS-0.22BP	70.0	14.8	52.7	8.1	0.8

Conductivity standard deviation δC (μS/cm). Diameter standard deviation δD (nm). Protein content standard deviation δP (%(w/w)).

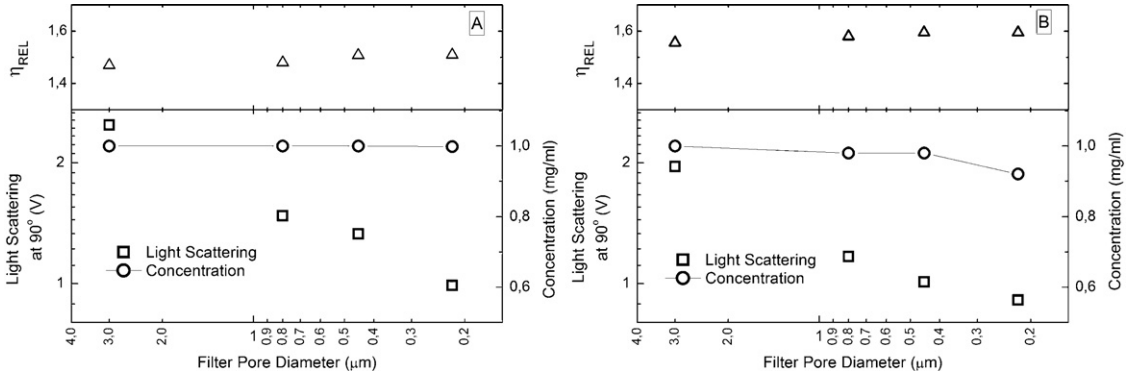

Fig. 3. TDSLS of Biotec A guar gum samples filtered through a series of cellulose ester membranes. (A) Relative viscosity × filtration pores (μm) graph, concentration (mg/ml) × filtration pores (μm) graph and LS signal intensity at 90° × filtration pores (μm) graph. (B) The same graphs for Sigma B guar gum.

ratio of peak area integration for mannose and galactose (Dea & Morrison, 1975) were the same (1.2:1) for samples GGB-NP, GGB-AP and GGB-0.22AP (spectra not shown for brevity sake). This high peak ratio found here means a high degree of substitution, and the presence of a highly soluble galactomannan (Dea, Clark, & Mccleary, 1986).

3.2. Sigma guar gum (GGS)

GPC results for non purified Sigma guar gum, purified Sigma A and B are seen in Table 1. Non purified Sigma guar presented two main peaks in its molar mass distribution; one of them presented several small convoluted peaks (graph not shown). The small convoluted peaks are related to small molecules eluted at a retention volume greater than 7.5 ml. This may be due to fragmentation of polysaccharides during their extraction (Sun, Fang, Kelly Goodwin, Lawther, & Bolton, 1998) or the presence of two different mixed batches of polysaccharides. It also showed a wide polydispersity and low column recovery 46%, which is a characteristic of insoluble aggregate presence.

3.2.1. Non-purified Sigma guar gum (GGS-NP)

Non purified Sigma guar gum shows a fiber network with spherical aggregates in between fibers and within then, as seen in Fig. 1G and H.

3.2.2. Purified Sigma guar gum (GGS-P)

Sigma guar gum was purified in two ways as described in Section 2. The average diameter measurements from AFM results, shown in Table 2, indicate that the fiber diameter produced with Sigma A is smaller than those produced by Sigma B. The reason for this is likely to be the difference in molar mass distribution, hydrodynamic radius and polydispersity index. All three reasons are a consequence of ethanol precipitation step procedure. Indeed, GPC results in Fig. 4, show that the two purification procedures generated evident differences in molecular distributions. It is known that ethanol dehydrates polysaccharides. In an aqueous solution, polysaccharide molecules are linked together through water molecules by hydrogen bonds. This keeps polysaccharide molecules water soluble. By adding ethanol, it will link preferentially to the water molecule, removing the water link between polysaccharides. Then they will get closer and precipitate. Therefore, adding pure ethanol into polysaccharide aqueous solution leads to precipitation of bigger molecular chains, leaving the smaller ones dispersed in the supernatant. Continuously washing with growing ethanol concentrations continuously removes smaller molecular chains. This leads to a final solution with a cumulative weight fraction shifted to higher molar mass, as shown in Fig. 4 for Sigma B samples. Otherwise, when adding the polysaccharide aqueous solution into pure ethanol, the excess ethanol will precipitate all molecules at once, regardless of their molecular chain size. This leads to a final solution with a cumulative weight fraction shifted to lower molar mass, as shown in Fig. 4 for Sigma A samples. Fig. 4 shows that Sigma B has less *cumulative* weight fraction for molar mass varying from 4.8 to 5.75 ($\log M_w$) than Sigma A. Biotec B follows the same trend. It means that pouring ethanol on the polysaccharide solution, as done for Sigma B, does not favor the precipitation of low mass molecules. Sigma A is slightly more polydisperse, has smaller polymer chains, and smaller hydrodynamic volume. This produces lower local chain entanglement density and may be responsible for differences in diameters and even in break-up of local chain-to-chain coupling, resulting in droplet formation (Gupta, Elkins, Long, & Wilkes, 2005).

3.2.2.1. Purified GGS- BP successively filtered through decreasing pore size. As can be observed in Fig. 5, when visually comparing fiber network morphology in Fig. 5A (GGS-NP) and Fig. 5C (GGS-BP), we noticed that the aggregation excess disappeared for purified samples. Only a few remaining aggregates can be observed.

Furthermore, as the solutions are sequentially filtered, the fiber homogeneity continually improves, as seen in Fig. 5E, G and I. The spherical aggregations, which are visible within the fiber structure obtained with an unfiltered solution (Fig. 6A), disappear when successively filtered with 0.8 and 0.45 μm pore membranes, as shown in Fig. 6B.We noticed the same trends of fiber diameter reduction, LS reduction, constant viscosity and constant concentration with filtration already observed for Biotec guar gum, as shown in Table 2

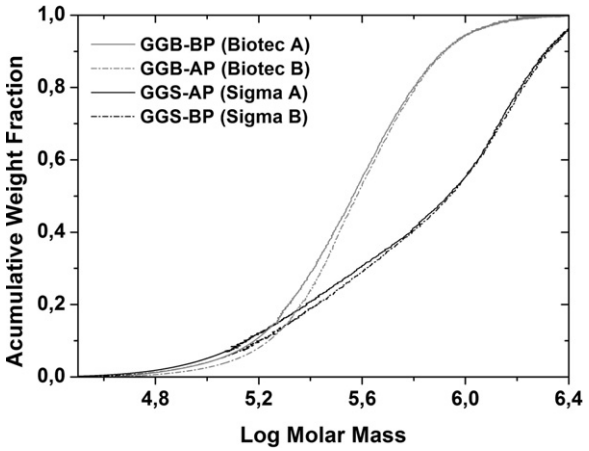

Fig. 4. Cumulative weight fraction × log molar mass for GGS-AP (black line), GGS-BP (black dash dot), GGB-AP (gray line) and GGB-BP (gray dash dot).

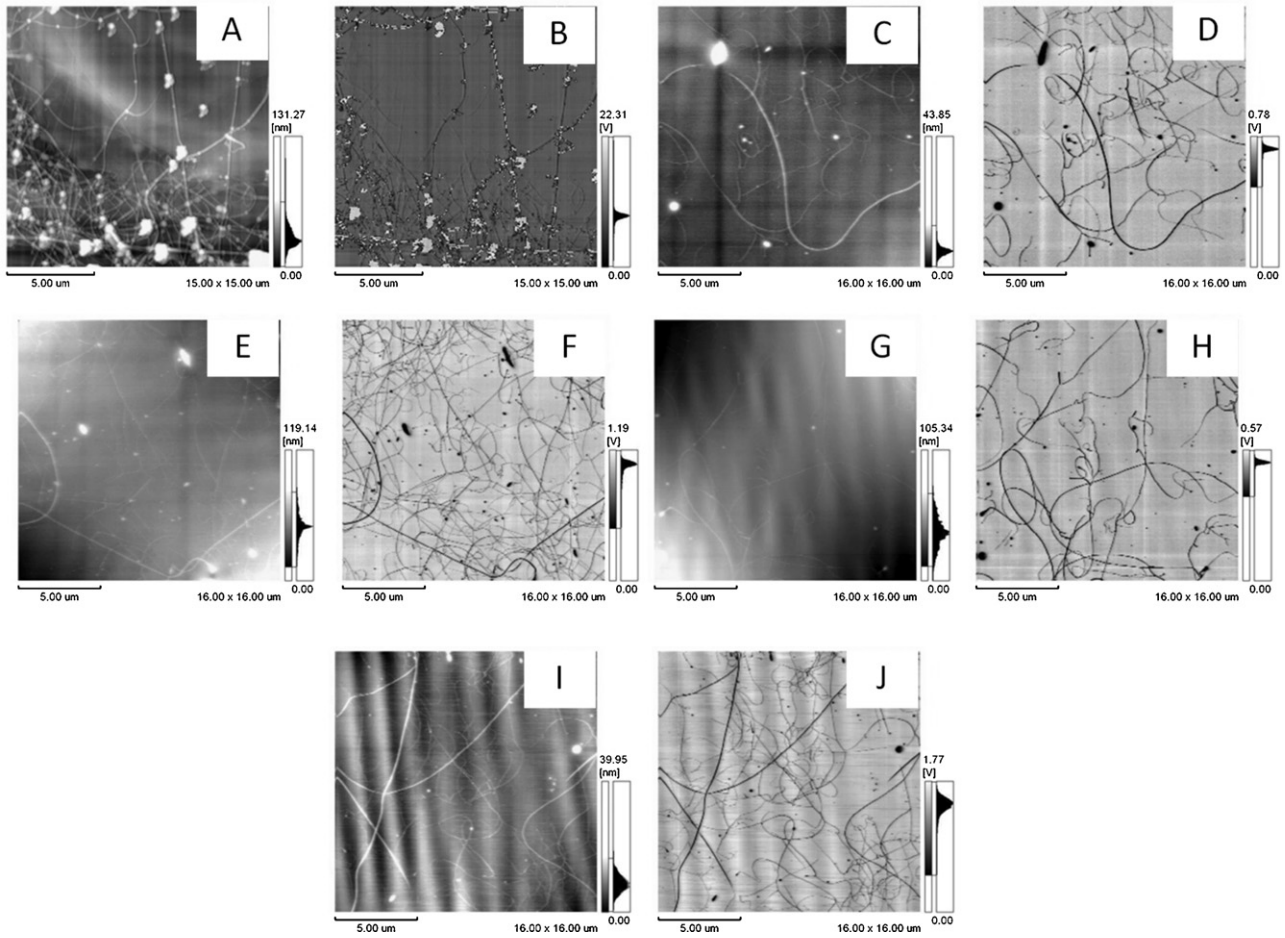

Fig. 5. (A) AFM image in dynamic mode (15.00 × 15.00) μm of GGS-NP 1% (w/w) deposited by electrospinning. (B) Phase image of (A). (C) AFM image in dynamic mode (16.00 × 16.00) μm of 1% (w/w) GGS-BP. (D) Phase image of (C), (E). AFM image in dynamic mode (16.00 × 16.00) μm of 0.8 μm filtered GGS-BP 1% (w/w). (F) Phase image of (E). (G) AFM image in dynamic mode (16.00 × 16.00) μm of 0.45 μm filtered GGS-BP, 1% (w/w). (H) Phase image of (G). (I) AFM image in dynamic mode (16.00 × 16.00) μm of 0.22 μm filtered GGS-BP 1% (w/w). (J) Phase image of (I). Experimental conditions for (A), (C); 0.52 kV/cm, feed rate 9.3 μl/min and (E), (G), (I) 0.5 kV/cm, feed rate 9.3 μl/min.

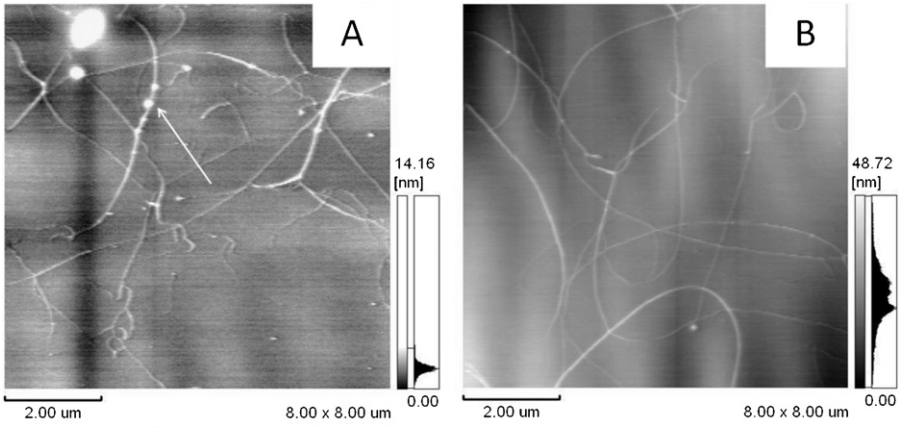

Fig. 6. AFM dynamic mode image of GGS-BP 1% (w/w) deposited by electrospinning. (A) AFM dynamic mode image (8.00 × 8.00) μm of GGS-BP 1% (w/w). (B) AFM dynamic mode image (8.00 × 8.00) μm of GGS-BP 1% (w/w), filtered successively with 0.8, 0.45 cellulose membrane. Fibers are more homogeneous and aggregates disappear after filtering solution. Experimental conditions for (A) 0.52 kV/cm, feed rate 9.3 μl/min. (B) 0.5 kV/cm, feed rate 9.3 μl/min.

and Fig. 2. It confirms that the filtration process yields the same results for both materials.

3.2.2.2. NMR results. The NMR results for samples GGS-NP, GGS-BP and GGS-0.2BP (spectra not shown), did not present any differences for both processes of purification and filtration. It was obtained the same Man:Gal ratio (1.2:1) as for Biotec.

4. Conclusion

We have being successful in electrospinning guar gums from two different commercial sources. The used gums have the same Man:Gal ratio, different average molar masses and polidispersity index. The solutions were prepared at several different concentrations starting from 1% (w/w).

The fibers obtained for raw product solutions were not uniform and presented aggregates between fibers and within them for both cases. This non-uniformity was mainly caused by the presence of insoluble aggregates. Furthermore, Sigma depositions had more pronounced presence of aggregates than Biotec. The differences between them are linked to higher average molar mass and polidispersity for Sigma guar gum.

Two different procedures were used for guar gum purification and a sequence of filtration with different pore sizes to enhance solution homogeneity and solubility. We verified that such procedures changed molar mass distribution. Depending on the precipitation step, within the purification procedure, different fiber diameters were obtained. The precipitation step, which produced polymers with higher *cumulative* low molar mass molecules, slightly bigger polydispersity, smaller polymer chains, and smaller hydrodynamic volume, yielded the smaller diameter electrospun fibers.

Filtration through a series of decreasing membrane pores reduced molecular aggregation. As a consequence, the fiber homogeneity was enhanced, the presence of aggregates was reduced and fiber diameter decreased for both cases. We also noticed an appreciable electric field reduction to achieve electrospinning after filtration.

Acknowledgments

The authors acknowledge the INCT for Diagnostics in Public Health/CNPQ, CAPES (Rede Nanobiotec) and CNPq for funding and BIOPOL/UFPR, MFA/UFPR and LITS/UFPR for material support.

References

Agarwal, S., Wendorff, J. H., & Greiner, A. (2008). Use of Electrospinning technique for biomedical applications. *Polymer*, *49*, 5603–5621.

Bourbon, A. I., Pinheiro, A. C., Ribeiro, C., Miranda, C., Maia, J. M., Teixeira, J. A., et al. (2010). Characterization of galactomannans extracted from seeds of *Gleditsia triacanthos* and *Sophora japonica* through shear and extensional rheology: Comparison with guar gum and locust bean gum. *Food Hydrocolloids*, *24*, 184–192.

Cheng, Y., Prud'homme, R. K., Chik, J., & Rau, D. C. (2002). Measurements of forces between galactomannan polymer chains: Effect of hydrogen bonds. *Macromolecules*, *35*, 10155–10161.

Cunha, P. L. R., de Paula, R. C. M., & Feitosa, J. P. A. (2007). Purification of guar gum for biological applications. *Biological Macromolecules*, *41*, 324–331.

Dea, I. C. M., Clark, A. H., & Mccleary, B. V. (1986). Effect of galactose-substitution-patterns on the interaction properties of galactomannans. *Carbohydrate Research*, *147*, 275–294.

Dea, I. C. M., & Morrison, A. (1975). Chemistry and interactions of seed galactomannans. *Advances in Carbohydrate Chemistry and Biochemistry*, *31*, 241–312.

Duvail, J. L., Retho, P., Garreau, S., Louarn, G., Godon, C., & Demoustier-Champagne, S. (2002). Transport and vibrational properties of poly(3,4-ethylenedioxythiophene) nanofibers. *Synthetic Metals*, *131*, 123–128.

Engel, A., Schoenenberger, A.-C., & Müller, D. J. (1997). High resolution imaging of native biological sample surfaces using scanning probe microscopy. *Current Opinion in Structural Biology*, *7*, 279–284.

Freitas, R. A., Drenski, M. F., Alb, A. M., & Reed, W. F. (2010). Characterization of stability, aggregation, and equilibrium properties of modified natural products; the case of carboxymethylated chitosans. *Materials Science and Engineering C*, *30*, 34–41.

Ganter, J. L. M. S., Milas, M., Corrêa, J. B. C., Reicher, F., & Rinaudo, M. (1992). Study of solutions properties of galactomannan from the seeds of *Mimosa Scabrella*. *Carbohydrate Polymers*, *17*, 171–175.

Gittings, M. R., Cipelletti, L., Trappe, V., Weitz, D. A., In, M., & Marques, C. (2000). Structure of guar in solutions of H_2O and D_2O: An ultra-small angle light scattering study. *Journal of Physical Chemistry B*, *104*, 4381–4386.

Gomez, C., Navarro, A., Manzanares, P., Horta, A., & Carbonell, J. V. (1997). Physical and structural properties of barley.(1 > 3) (1 > 4)-β-D-glucan. Part 1. Determination of molecular weight and macromolecular radius by light scattering. *Carbohydrate Polymers*, *32*, 7–15.

Greiner, A., & Wendorff, J. H. (2007). Electrospinning: A fascinating method for the preparation of ultrathin fibers. *Angewandte Chemie*, *46*, 5670–5703.

Gupta, P., Elkins, C., Long, T. E., & Wilkes, G. L. (2005). Electrospinning of linear homopolymers of poly(methyl methacrylate): Exploring relationships between fiber formation, viscosity, molecular weight and concentration in a good solvent. *Polymer*, *46*, 4799–4810.

Gupta, P., & Wilkes, G. L. (2003). Some investigations on the fiber formation by utilizing a side-by-side bicomponent electrospinning approach. *Polymer*, *44*, 6353–6359.

Hartree, E. F. (1972). Determination of protein: A modification of the Lowry method that gives a linear photometric response. *Analytical Biochemistry*, *48*, 422–427.

Kenawy, E. R., Ayman, J. M., Watkins, J. R., Bowlin, G. L., Matthews, J. A., & Simpson, D. G. (2003). Electrospinning of poly(ethylene-co-vinyl alcohol) fibers. *Biomaterials*, *4*, 907–913.

Lang, P., & Kajiwara, K. (1993). Investigations of the architecture of tamarind seed polysaccharide in aqueous solution by different scattering techniques. *Journal Biomaterial Science and Polymer Edition*, *4*, 517–528.

Lee, K. Y., Jeong, L., Kang, Y. O., Lee, S. J., & Park, W. H. (2009). Electrospinnig of polysaccharides for regenerative medicine. *Advanced Drug Delivery Reviews*, *61*, 1020–1032.

Li, W., Wan, Q., Cui, S. W., Huang, X., & Kakuda, Y. (2006). Elimination of aggregates of (1 > 3),(1 > 4)-β-D-glucan in dilute solutions for light scattering and size exclusion chromatography study. *Food Hydrocolloids*, *20*, 361–368.

Liu, D., Zhang, H., Grim, P. C. M., De Feyter, S., Wiesler, U. M., Berresheim, A. J., et al. (2002). Self-assembly of polyphenylene dendrimers into micrometer long nanofibers: An atomic force microscopy study. *Langmuir*, *18*, 2385–2391.

Ma, P. X., & Zhang, R. (1999). Synthetic nano-scale fibrous extracellular matrix. *Journal of Biomedical Materials Research*, *46*, 60–72.

Mark, H. F., Overberger, C. G., Othmar, D. F., & Seaborg, G. T. (2007). *Kirk-Othmer encyclopedia of chemical technology* (5th ed.). Hoboken: John Wiley & Sons. (Chapter 2).

Mccleary, B. V., Amado, R., Warbel, R., & Neukom, H. (1981). Effect of galactose content on the solution and interactions properties of guar and carob galactomannans. *Carbohydrate Research*, *92*, 269–285.

Nakata, K., Fujii, K., Ohkoshi, Y., Gotoh, Y., Nagura, M., Numata, M., et al. (2007). Poly(ethylene terephthalate) nanofibers made by sea-island-type conjugated melt spinning and laser-heated flow drawing. *Macromolecular Rapid Communications*, *28*, 792–795.

Newlin, T. E., Lovell, S. E., Saunders, P. R., & Ferry, J. D. (1962). Long-range intermolecular coupling in concentrated poly-n-butyl mathacrylate solutions and its dependence on temperature and concentration. *Journal of Colloid Science*, *17*, 10–25.

Nie, H., He, A., Zheng, J., Xu, S., Li, J., & Han, C. C. (2008). Effects of chain conformation and entanglement on the electrospinnig of pure alginate. *Biomacromolecules*, *9*, 1362–1365.

Ondarçuhu, T., & Joachim, C. (1998). Drawing a single nanofiber over hundreds of microns. *Europhysics Letters*, *42*, 215–220.

Picout, D. R., Ross-Murphy, S. B., Errington, N., & Harding, S. E. (2003). Pressure cell assisted solubilization of xyloglucans: Tamarind seed polysaccharide and detarium gum. *Biomacromolecules*, *4*, 799–807.

Pollard, M. A., Kelly, R., Fischer, P. A., Windhab, E. J., Eder, B., & Amado, R. (2008). Investigation of molecular weight distribution of LBG galactomannan for flours prepared from individual seeds, mixtures, and commercial samples. *Food Hydrocolloids*, *22*, 1596–1606.

Robinson, G., Ross-Murphy, S. B., & Morris, E. R. (1982). Viscosity–molecular weight relationships, intrinsic chain flexibility, and dynamic solution properties of guar galactomannan. *Carbohydrate Research*, *107*, 17–32.

Sassaki, G. L., Riter, D. S., Santana Filho, A. P., Guerrini, M., Lima, M. A., Cosentino, C., et al. (2011). A robust method to quantify low molecular weight contaminants in heparin: Detection of tris(2-n-butoxyethyl) phosphate. *Analyst*, *136*, 2330–2338.

Schiffman, J. D., & Schauer, C. L. (2008). A review: Electrospinning of biopolymer nanofibers and their applications. *Polymer Reviews*, *48*, 317–352.

Shenoy, S. L., Bates, W. D., Frisch, H. L., & Wnek, G. E. (2005). Role of chain entanglements on fiber formation during electrospinning of polymer solutions: Good solvent, non-specific polymer–polymer interaction limit. *Polymer*, *46*, 3372–3384.

Simkovic, I. (2008). What would be greener than composites made from polysaccharides? *Carbohydrate Polymers*, *74*, 759–762.

Stijnman, A. C., Bodnar, I., & Tromp, R. H. (2011). Electrospinning of food-grade polysaccharides. *Food Hydrocolloids*, *25*, 1393–1398.

Sun, R. C., Fang, J. M., Kelly Goodwin, A., Lawther, J. M., & Bolton, A. J. (1998). Fractionation and characterization of polysaccharides from abaca fibre. *Carbohydrate Polymers*, *37*, 351–359.

Talwar, S., Hinestroza, J., Pourdeyhimi, B., & Khan, S. A. (2008). Associative polymer facilitated electrospinning of nanofibers. *Macromolecules*, *41*, 4275–4283.

Vårum, K. M., Smidsrød, O., & Brant, D. A. (1992). Light scattering reveals micelle-like aggregation in (1 > 3),(1 > 4)-β-D-glucans from oat aleurone. *Food Hydrocolloids*, *5*, 497–511.

Wang, Q., Huang, X., Nakamura, A., Burchard, W., & Hallet, F. R. (2005). Molecular characterization of soybean polysaccharides: An approach by size exclusion chromatography, dynamic and static light scattering methods. *Carbohydrate Research*, *340*, 2637–2644.

Wientjes, R. H. W., Duits, M. H. G., Jongschaap, R. J. J., & Mellema, J. (2000). Linear rheology of guar gum solutions. *Macromolecules*, *33*, 9594–9605.